International Conference on Space Optics—ICSO 2020

Virtual Conference

30 March–2 April 2021

Towards a next-generation Earth Radiation Budget radiometer by optimization of the cavity geometry and coating

Towards a next-generation Earth Radiation Budget radiometer by optimization of the cavity geometry and coating

Luca Schifano[a,b], Lien Smeesters[b,c], Francis Berghmans[b,c], and Steven Dewitte[a]

[a]Royal Meteorological Institute of Belgium, Avenue Circulaire 3, Brussels, Belgium
[b]Vrije Universiteit Brussel, Department of Applied Physics and Photonics, Brussels Photonics (B-PHOT), Pleinlaan 2, Brussels, Belgium
[c]Flanders Make, Pleinlaan 2, Brussels, Belgium

ABSTRACT

Climate on Earth is determined by the Earth Radiation Budget (ERB), which quantifies the incoming and outgoing radiative energy fluxes at the top-of-atmosphere. The ERB can be monitored from space by non-scanning wide field-of-view radiometers, or by scanning narrow field-of-view radiometers. In this paper, we investigate the use of two wide field-of-view radiometers geometries, each of which composed of a baffle and precision aperture featuring a field-of-view of minimally of 127°, allowing to monitor the Earth's radiative fluxes from limb-to-limb, from an altitude of about 700 km. Our first radiometer composes a near-hemispherical cavity enabling a uniform angular sensitivity, in combination with a conical part and baffle to ensure a wide field-of-view. For the second radiometer design, we consider an integrating sphere supplemented with an active-cavity radiometer positioned at an angle of 90° from the precision aperture. Both designs are equipped with practical coating materials, i.e. Black Velvet for the near-spherical radiometer and Spectralon for the integrating sphere. For both designs, the cavity geometry is analyzed and an evaluation of the interior cavity coatings is made. To compare both designs, we evaluate the optical absorbance by relying on scattering analyses. To conclude, we present an evaluation of both radiometer designs, comprising an analysis of the coating properties, giving valuable input for the next-generation Earth Radiation Budget radiometers.

Keywords: Earth Radiation Budget; Earth Energy Imbalance; Space instrumentation; Radiometer; Integrating sphere; Optical modelling; Coating; Black Velvet; Spectralon.

1. INTRODUCTION

The radiative energy fluxes at the top-of-atmosphere (TOA) are described by the Earth Radiation Budget (ERB),[1] which plays a major role in the climate system. In fact, global warming is caused by the Earth Energy Imbalance (EEI), a small but non-zero net energy remaining in the Earth's system, caused by an increasing amount of greenhouse gases in the atmosphere due to anthropogenic activity. This is one of the most crucial parameters to be monitored in our pursuit to understand climate change.[2–4]

The earliest measurements of the ERB were made in 1984 using wide field-of-view radiometers, allowing to observe the Earth from limb to limb.[5] This measurement principle has been adapted during the Earth Radiation Budget Experiment (ERBE),[6] where the low resolution ERB measurements obtained using WFOV radiometers were compared with the higher resolution measurements from the scanning radiometers. In addition, these scanning radiometers avoided the thermal offset problems of WFOV radiometers.[7] Therefore, the CERES program continued with scanning radiometers[7,8] However, WFOV radiometers have gained renewed interest recently, as illustrated with the development of the SIMBA[9] and RAVAN[10] 3U CubeSats.

As a SIMBA follow-on satellite, we propose a new concept to measure the radiative fluxes at the TOA, using a combination of space-based instruments. The first instrument is a WFOV radiometer, which aims to measure

accurately the total Earth's outgoing energy.[11] This radiometer is supplemented with high-resolution shortwave (SW, [400–1100] nm),[12] and longwave (LW, [8–14] μm) WFOV cameras, improving the radiometer accuracy, increasing the spatial resolution, and enbabling the spectral separation between Reflected Solar Radiation (RSR) and Outgoing Longwave Radiation (OLR).

This paper compares the design and performance of 2 WFOV radiometer configurations: (1) our in-house developed cavity radiometer of which the interior is coated with Black Velvet and (2) an integrating sphere design measuring radiation after multiple-reflections on the interior Spectralon coating. Both radiometer designs are simulated using ASAP®, Brault Research, including an evaluation of the cavity losses and absorbance.

2. METHODS

We target the development of an optical model enabling to study the outgoing flux of the cavity radiometer and integrating sphere, here defined as the flux that is lost without contributing to the detected signal. Since in this model, the source is placed at the entry of the cavity, a way to determine the flux leaving the cavity is to put a virtual detector just below the cavity. Therefore, in a first step, in Section 2.1, the geometry of our measurement instrument is defined. Following, the source models are inserted, as presented in Section 2.2. Third, in Section 2.3, the properties of the considered coating materials, Black Velvet and Spectralon are discussed. Finally, we investigate possible ways to optimize the cavity radiometer and the integrating sphere 2.4.

2.1 Geometry

Our cavity radiometer geometry builds on the knowledge of previously developed radiometers. Prior to the monitoring of the Earth's radiation budget with WFOV radiometers, the first radiometers were used for Total Solar Irradiance monitoring, and were developed in different geometries, such as a cone shape (ACRIM,[13] TIM[14]), an inverted cone shape (PMO[15]), or a cylinder (DIARAD[16]). Our cavity radiometer is an improvement of the cavity radiometer from the Sun-Earth IMBAlance (SIMBA) mission,[17] developed at the Royal Meteorological Institute of Belgium, and which inherited its measurement principle using electrical substitution from the DIARAD-type radiometer. Thanks to its novel cavity shape, our radiometer features a wide field-of-view of 135°, exceeding the 127° that is required to observe the Earth from limb-to-limb from a nominal altitude of 700 km, enabling to monitor the Earth's total outgoing radiation while allowing for pointing errors. This radiometer and its functioning are described in detail in.[11] The cavity is composed of a near-hemispherical part and a conical part supplemented with an appropriate baffle. In our model, the diameter of the cavity aperture equals 6 mm. Below the cavity radiometer, there is a baffle featuring a precision aperture with a diameter of 5 mm. The cavity radiometer aperture is slightly larger than the precision aperture to allow for alignment errors, ensuring that no radiation is stopped by the cavity aperture.

An alternative to the cavity radiometer is to use an integrating sphere, which features an easier geometry. Also, an integrating sphere offers the advantage to enable a stronger versatility, e.g. placing a spectrometer at the detector or using filters in front of the entrance aperture. Here, we use a full sphere with a standard size of 5 cm of diameter. The entrance aperture equals 1 mm diameter, while the detection area equals a circular area with a diameter of 1 cm. These pameters have been determined according to best practices, i.e. targeting to obtain a port fraction $f \approx 0.01$, , as to achieve an optimal performance of the integrating sphere.[18] Therefore, we have:

$$f = \frac{A_e + A_d}{A_s} = \frac{\pi(0.5^2 + 5^2)}{4\pi(25^2)} = 0.0101 \approx 0.01 \tag{1}$$

where A_e is the area of the entrance aperture, A_d is the area of the detector, and A_s is the area of the sphere.

A major difference with the cavity radiometer is that the latter has been shaped solely in the purpose of observing the Earth from limb to limb, without needing for an interior baffle. While for the integrating sphere, an interior baffle is needed in the case of Earth observation, to avoid that incoming radiation falls directly onto the detector.

2.2 Sources

Two pointing modes, therefore two cases, are considered: Solar radiation and Earth's radiation (Figure 1). Solar radiation is only used for calibration purposes. This source can be modeled as a 5 mm diameter beam (since it passes through the precision aperture first) entering the aperture of the cavity, with a full emission angle of 3°. Regarding the Earth's emitted radiation, we consider a Lambertian source[19] with an emission angle of 127°, corresponding with the acception angle of the baffle.

Total Solar Irradiance: 1362 W/m²
Incoming: 340.4 ± 0.2 W/m²

SUN

Total Earth's Outgoing Irradiance

Reflected (SW): 101.5 ± 2.7 W/m²
Emitted (LW): 238.0 ± 2.0 W/m²

EARTH

SIMBA follow-on
satellite, comprising our novel radiometer

WFOV
135°

Earth Energy Imbalance

EEI = Incoming – Reflected (SW) – Emitted (LW)
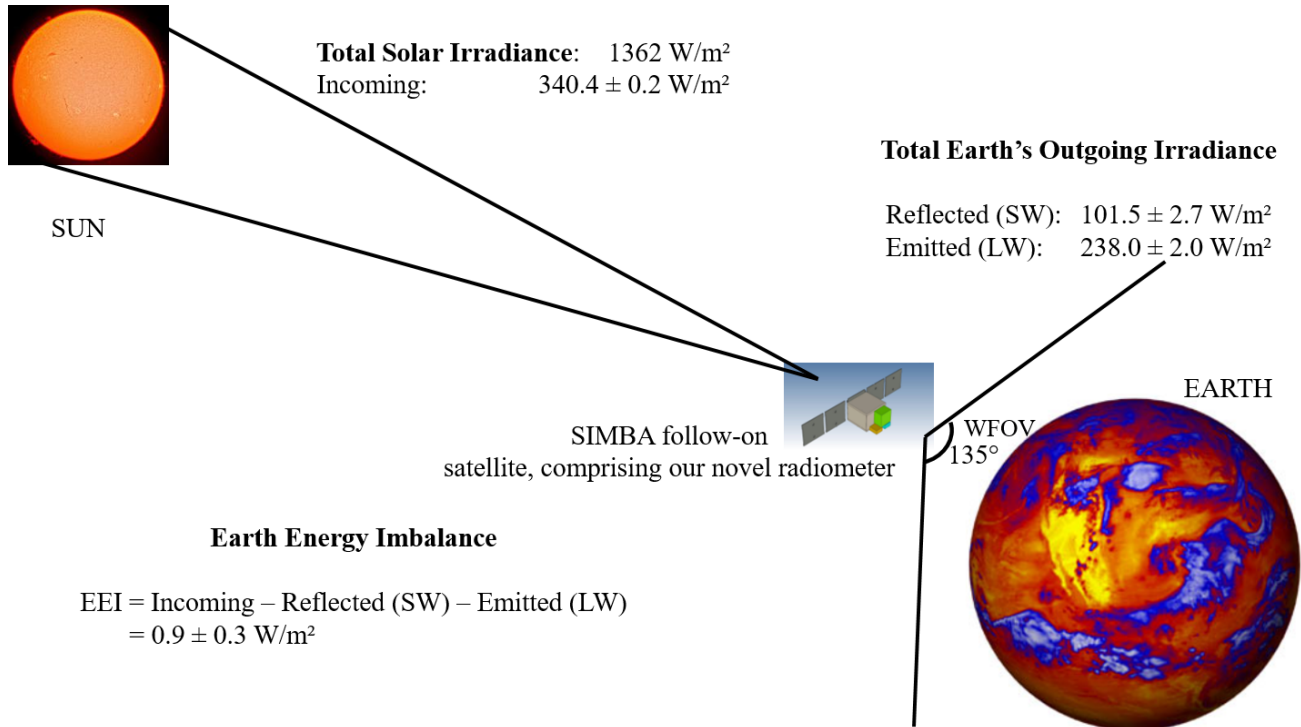= 0.9 ± 0.3 W/m²

Figure 1. Earth viewed by the WFOV radiometer. Occasional Solar pointing will allow intercalibrating the Incoming Solar Radiation and the Earth's Total Outgoing Radiation measurements. SW stands for *shortwave* and LW for *longwave*.

2.3 Coating and absorption factor

The interior cavity walls of the radiometer are coated with Black Velvet, a black paint, that allows to absorb incoming radiation.[20] The absorption factor of Black Velvet equals 0.97 +/- 0.01, for both spectral regions of interest (SW and LW), and considering perpendicular illumination. Also, we consider three illumination cases: (1) LW Earth, for which a Lambertian source of 127° is simulated in the 8 μm – 14 μm spectral range; (2) SW Earth, featuring the same angle but considering the 400 nm – 1100 nm spectral range; (3) Solar, a SW source with an emission angle of incidence of ±1.5°. This definition implies that all generated rays will first encounter the hemispherical part of the cavity, since the source rays are only defined with a total emission angle of 127°, while the conical part of the cavity features a larger acceptance angle of 135°. For this analysis performed in ASAP®, Breault Research, we use the commands SPLIT 2 for specular reflection and LEVEL 2 for scattered light, a total flux of 100 (in arbitrary units), and 50000 rays.

Considering the integrating sphere, a space-based Spectralon® coating from LabSphere is considered.[21] This coating features a diffuse reflectance higher than 99% (scattering) until 250 nm, then decreases to 95% until 2500 nm (Figure 2). In our simulations, we will assume 99% of diffuse reflectance and 1% of absorption, to see if the integrating sphere has a better performance than the cavity radiometer, even in certain spectral regions of interest only. In addition, a second simulation with 100% of scattering will be done to assess the influence of the geometry only. For this analysis, we use the command LEVEL 750 for scattered light, while with the HALT command we allow 10^{18} interactions between the rays and the coating, in order to avoid that the lights are wrongly trapped in the integrating sphere.
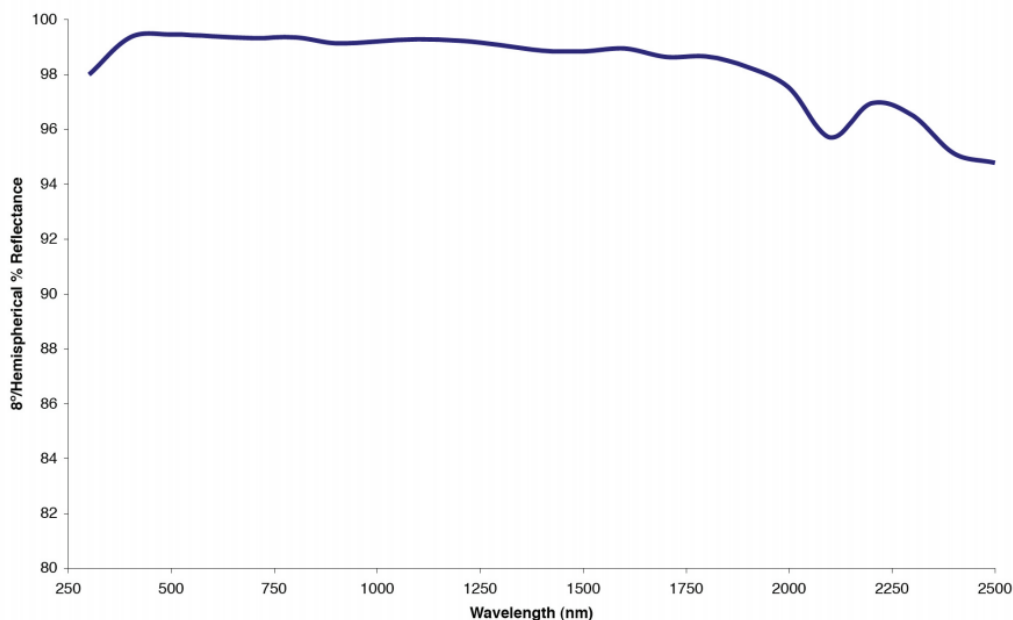

Figure 2. Typical 8° Hemispherical Reflectance (SRM-990) of the Space-grade Spectralon® Reflectance Material, between 250 nm and 2500 nm.[21]

2.4 Optimization

Both the cavity radiometer and integrating sphere were optimized towards minimal light loss. Specifically, the optimization targets to minimize the light flux leaving the cavity by considering the flux at the detector surface, positioned at the entrance of the geometry, as merit function.

Considering the cavity radiometer, our initial design composed a perfect hemispherical cavity, supplemented with a bottom conical part. After including the coating in the design, optimization of the hemispherical part was done, by considering its semi-length along the Z-axis as variable. Considering the integrating sphere, an optimization is performed when considering the size of the entrance aperture and detector area as variables, relatively to the size of the sphere.

3. RESULTS

This section is composed of two parts: the first part is dedicated to the simulations of the cavity radiometer, whilst the second part focuses on the integrating sphere. For both parts, an outlook of the model is given and the results of the analysis and optimization are discussed.

3.1 Cavity radiometer

The investigation on the geometry and the coating of the cavity radiometer was the object of a precedent paper,[22] of which the key results will be repeated for benchmarking purposes. Considering a total Earth's

outgoing radiative flux of 340 W/m² (Figure 1), Table 1 gives the relative and absolute outgoing fluxes when observing the Earth and the Sun from space. In all cases, the outgoing flux is less than 1 W/m². This excellent result originates from a combined effect from the optimized geometry and good coating properties. In fact, the cavity geometry has been designed solely in this purpose. An optimization has been performed on that cavity geometry, and the results show that the initial geometry (Figure 3) performed the best. In comparison to pure flat sensors, the coating absorption factor is of less importance when associated with a proper cavity geometry. In fact, a purely flat sensor coated with Black Velvet would absorb 97% of the incoming flux, resulting in a loss of 10.2 W/m² when observing the Earth (in the SW range, which is the best case scenario), indicating the importance of the optimized radiometer geometry.
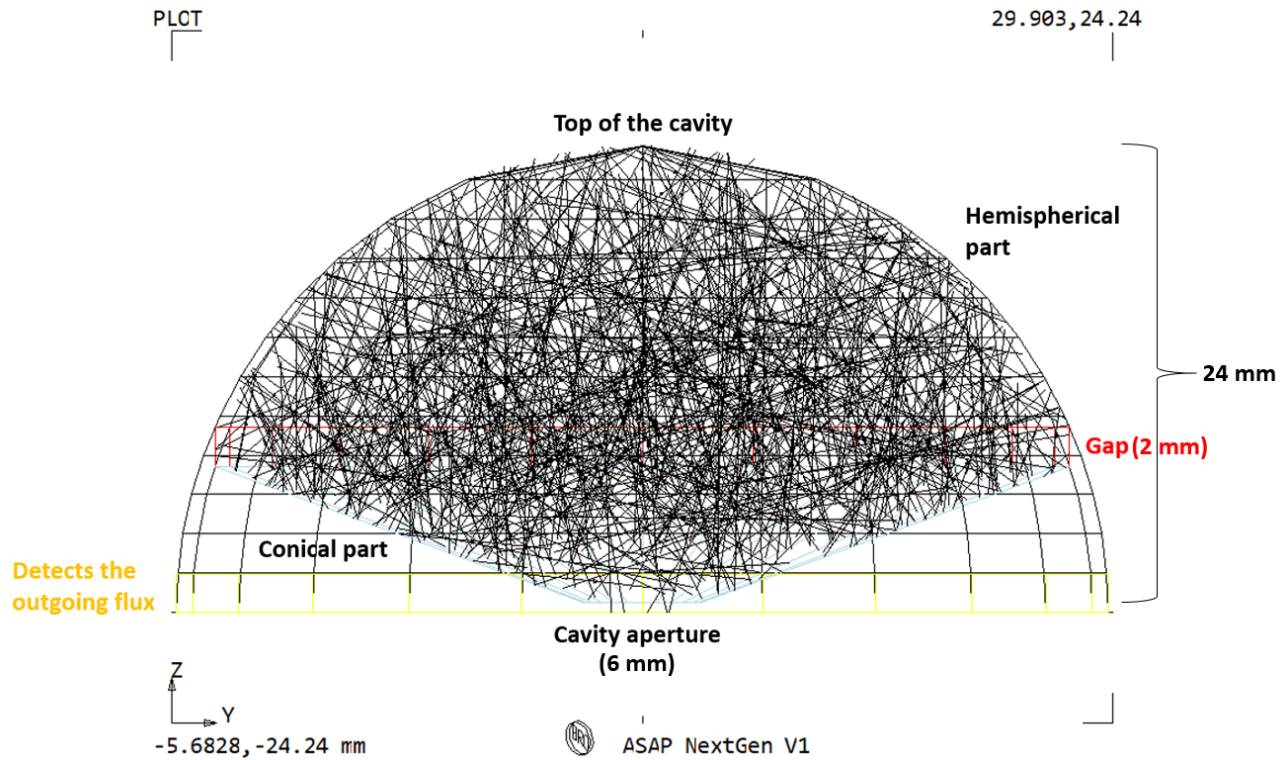

Figure 3. The cavity radiometer is composed of a hemispherical part, a conical part, and has an aperture where the radiation is entering. In our ASAP model, the gap of 2 mm between the hemispherical part and the conical part is an absorptive layer that stops the propagation of light (in red). In yellow, another absorptive structure intercepts the outgoing light. The source has an emission angle of 127° to illustrate the Earth's case. Rays are plotted in black.

Table 1. Computed outgoing flux (in % of the incoming flux) for the cavity radiometer model with the gap, when applying a Black Velvet coating, when measuring Earth's radiation (SW and LW) and Solar calibration. The absolute outgoing flux is the light loss when observing Earth from space, considering a total Earth's outgoing radiative flux of 340 W/m².

	Relative outgoing flux	Absolute outgoing flux
Earth	0.2528%	0.86 W/m²
Sun	0.2195%	0.2746 W/m²

3.2 Integrating sphere

We investigate the integrating sphere as a possible alternative for the cavity radiometer, since integrating spheres are generally used in laboratory to measure radiation, and thus might offer a valuable alternative. The model for our integrating sphere is illustrated in Figure 4.
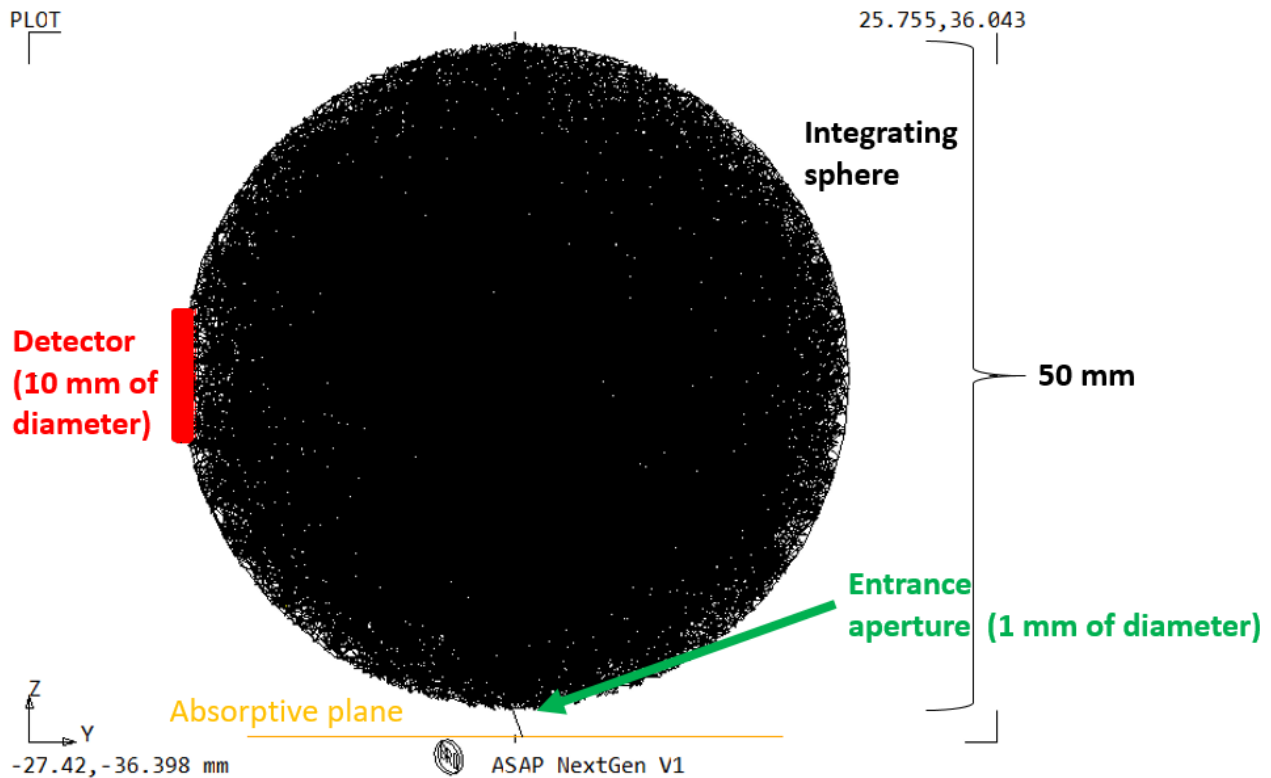

Figure 4. The integrating sphere. The rectangle (red) at the left is the detector measuring the signal. The yellow plane at the bottom quantifies the outgoing flux. The source, placed at the entrance of the integrating sphere, has a full emission angle of 127° and a diameter of 1 mm. Rays are plotted in black.

In our simulations, the Spectralon coating is 1% absorbing, while 99% of the incoming rays are scattered. The total light loss of the integrating sphere is, however, the superposition of the light that is escaping by the entrance aperture due to the geometry and the light that is absorbed by the coating. Despite the fact that the Spectralon absorption seems only a minor percentage, this shows to be a major contributing factor due to the multiple reflections on the interior of the integrating sphere (typically 24347 interactions until the end of the simulation). Consequently, in this case, the outgoing flux due to the geometry and the light absorption by the Spectralon are studied separately to identify their individual contributions. Specifically, when determining the geometrical influences, we investigated the outgoing flux and the detected flux, as indicated by the detectors in Figure 4, in case we consider 0% of light absorption by the Spectralon. Following, the influence of the Spectralon absorption is studied, by including the 1% absorption and studying again the outgoing and detected flux. Both of these cases where considered for Earth and Solar observation, giving rise to the results presented in Tables 2. Comparing Table 2 to Table 1, it shows that in all cases, even when considering the infuence of the geometry only, the flux reaching the detector is smaller than when using the cavity radiometer.

Table 2. Distribution of fluxes for the integrating sphere **with interior baffle and a coating with 1% and 0% of absorption**. The flux is whether absorbed by the sphere and the baffle, outgoing or detected. The observation cases are Earth observation and Solar calibration. The flux is relative and expressed in %.

	Coating 1% Earth	Coating 1% Sun	Coating 0% Earth	Coating 0% Sun
Absorbed	46.93	46.85	0.0258	0.0278
Outgoing	0.47	0.45	0.86	0.86
Detected	52.60	52.70	99.12	99.12

Considering Solar illumination, an optimization was carried out on the angle of incidence of the source, showing that the best results are found for a collimated input beam. Additionally, the merit function is reaching its minimum when the source is tilted with a small angle of -0.4°. However, it should be noted that the flux gain is very low, even negligible.

4. CONCLUSION

This paper compares the optical detected flux of 2 space instrumentation designs targeting to measure the radiative fluxes at the top-of-atmosphere, pursuing climate change monitoring in future space missions. The first instrument is a cavity radiometer coated with Black Velvet, designed in the only purpose to fulfill the requirements of this space mission. The second instrument is an integrating sphere coated with Spectralon, commonly used to measure radiation in laboratory. To compare both instruments, we analyze the flux that is detected by both instruments, and the flux that is lost at the end of the experiment. Besides, for both configurations, the detected light flux is studied both in case of Earth observation and Solar calibration. As a result of this study, we can observe that for both pointing modes the cavity radiometer is showing the best performance, indicating losses less than 0.26%. However, this design shows a higher complexity and less flexibility towards integration, while the integrating sphere is off-the-shelf available and enable to tailor the detector type towards the mission needs.

ACKNOWLEDGMENTS

REFERENCES

[1] Dewitte, S. and Clerbaux, N., "Measurement of the earth radiation budget at the top of the atmosphere - a review," *Remote Sensing* **9**, 1143 (2017).

[2] Hansen, J., Sato, M., Kharecha, P., and von Schuckmann, K., "Earth's energy imbalance and implications," *Atmospheric Chemistry and Physics* **11**, 13421–13449 (2011).

[3] Trenberth, K., Fasullo, J., von Schuckmann, K., and Cheng, L., "Insights into earth's energy imbalance from multiple sources," *Journal of Climate* **29**, 7495–7505 (2016).

[4] vonSchuckmann, K., Palmer, M., Trenberth, K., Cazenave, A., Chambers, D., Champollion, N., Hansen, J., Josey, S., Loeb, N., Mathieu, P., Meyssignac, B., and Wild, M., "An imperative to monitor earth's energy imbalance," *Nature Climate change* **6**, 138–144 (2016).

[5] Smith, G., Gibson, G., and Harrison, E., "History of earth radiation budget at langley research center," *8th History Symposium, American Meteorological Society* (2010).

[6] Barkstrom, B., "The earth radiation budget experiment," *BAMS* **5**, 1170–1185 (1984).

[7] Wong, T., Smith, G., Kato, S., Loeb, N., Kopp, G., and Shrestha, A., "On the lessons learned from the operations of the erbe nonscanner instrument in space and the production of the nonscanner toa radiation budget data set," *IEEE TGARS* **56(10)**, 5936–5947 (2018).

[8] Wielicki, B., Barkstrom, B., Harrison, E., III, R. L., Smith, G., and Cooper, J., "Clouds and the earth's radiant energy system (ceres): An earth observing system experiment," *BAMS* **77**, 853–868 (1996).

[9] Dewitte, S., Chevalier, A., Meftah, M., Kerschen, G., and Karatekin, O., "The sun-earth imbalance radiometer for a direct measurement of the net heating of the earth," *The 4S Symposium 2014* (2014).

[10] Swartz, W., Lorentz, R., Papadakis, S., Huang, P., Smith, A., Deglau, D., Yu, Y., Reilly, S., Reilly, N., and Anderson, D., "Ravan: Cubesat demonstration for multi-point earth radiation budget measurements," *Remote Sensing* **11(7)**, 796 (2019).

[11] Schifano, L., Smeesters, L., Geernaert, T., Berghmans, F., and Dewitte, S., "Design and analysis of a next-generation wide field-of-view earth radiation budget radiometer," *Remote Sensing* **12(3)**, 425 (2020).

[12] Schifano, L., Smeesters, L., Berghmans, F., and Dewitte, S., "Optical system design of a wide field-of-view camera for the characterization of earth's reflected solar radiation," *Remote Sensing* **12(16)**, 2556 (2020).

[13] Willson, R., "Active cavity radiometer type iv," *Applied Optics* **18(2)**, 179–188 (1979).

[14] Kopp, G. and Lawrence, G., "The total irradiance monitor (tim): instrument design," *Solar Physics* **230(1-2)**, 91–109 (2005).

[15] Brusa, R. and Frölich, C., "Absolute radiometers (pmo6) and their experimental characterization," *Applied Optics* **25(22)**, 4173–4180 (1986).

[16] Crommelynck, D. and Dewitte, S., "Metrology of total solar irradiance monitoring," *Advances in Space Research* **24(2)**, 195–204 (1999).

[17] ESA, "Simba CubeSat to swivel from Earth to Sun to help track climate change." ESA, 2020 https://www.esa.int/Enabling_Support/Space_Engineering_Technology/Simba_CubeSat_to_swivel_from_Earth_to_Sun_to_help_track_climate_change. (Accessed: 22 January 2021).

[18] LabSphere, "Integrating Sphere Theory and Applications." LabSphere, 2017 https://www.labsphere.com/site/assets/files/2551/integrating_sphere_theory_apps_tech_guide.pdf. (Accessed: 22 January 2021).

[19] Tu, L., Qin, Z., and Yand, L., "Identifying the lambertian property of ground surfaces in the thermal infrared region via field experiments," *Remote Sensing* **9**, 481 (2017).

[20] Adibekyan, A., Kononogova, E., Monte, C., and Hollandt, J., "High-accuracy emissivity data on the coatings nextel 811-21, herberts 1534, aeroglaze z306 and acktar fractal black," *International Journal of Thermophysics* **38(6)**, 89 (2017).

[21] LabSphere, "Space-Grade Spectralon® Diffuse Reflectance Material." LabSphere, 2021 https://www.labsphere.com/labsphere-products-solutions/materials-coatings-2/coatings-materials/space-grade-spectralon-diffuse-reflectance-material/. (Accessed: 22 January 2021).

[22] Schifano, L., Smeesters, L., Meulebroeck, W., Berghmans, F., and Dewitte, S., "Vacnt versus black velvet: a coating analysis for the next-generation earth radiation budget radiometer," in [*Remote Sensing of Clouds and the Atmosphere XXV*], **11531**, 115310J, International Society for Optics and Photonics (2020).